

Technical communication

Cite

Serna JDC, Ramos VM, Cabral-Costa JV, Vilas-Boas EA, Amaral AG, Ohya G, Caldeira da Silva CC, Kowaltowski AJ (2022) Measuring mitochondrial Ca^{2+} efflux in isolated mitochondria and permeabilized cells. MitoFit Preprints 2022.21. <https://doi.org/10.26124/mitofit:2022-0021>

Author contributions

Data collection and analysis was performed by JDCS, JVCC, VMR, EAVB, AGA, GO and CCCS. All authors wrote the manuscript. VMR contributed all art work. JDCS and AJK conceived and designed the framework of the manuscript.

Conflicts of interest

The authors declare they have no conflict of interest.

Received 2022-05-13

Accepted 2022-05-16









Online 2022-05-24

Data availability

Data available Open Access <https://doi.org/10.26124/mitofit:2022-0021>

Keywords – mitochondria; Ca^{2+} efflux; NCLX; mPTP; liver.

Measuring mitochondrial Ca^{2+} efflux in isolated mitochondria and permeabilized cells

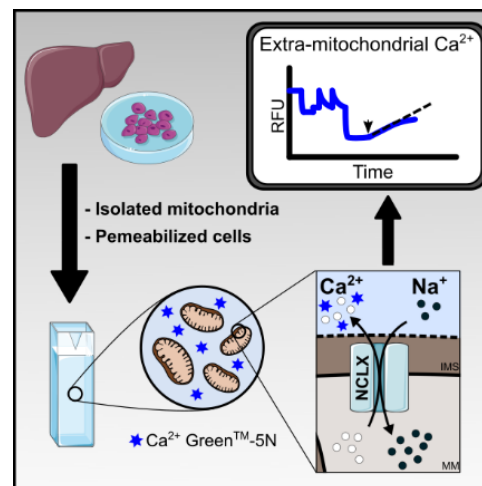
 Julian D. C. Serna¹,  Vitor de Miranda Ramos¹,  João Victor Cabral-Costa¹,  Eloisa A. Vilas-Boas¹,  Andressa G. Amaral²,  Georgia Ohya¹,  Camille C. Caldeira da Silva¹,  Alicia J. Kowaltowski^{1,*}

¹Departamento de Bioquímica, Instituto de Química, Universidade de São Paulo, 05508-900, Brazil.

²Departamento de Fisiologia, Instituto de Ciências Biomédicas, Universidade de São Paulo, 05509-900, Brazil.

* Corresponding author: alicia@iq.usp.br

Abstract



Mitochondrial Ca^{2+} efflux is essential for mitochondrial and cell Ca^{2+} homeostasis.

Mitochondrial inner membrane $\text{Ca}^{2+}/\text{H}^{+}$ and $\text{Na}^{+}/\text{Li}^{+}/\text{Ca}^{2+}$ (NCLX) exchangers are known today to be plastic transporters, with important roles in

physiological responses and pathological states. Until now, however, no consensus protocols were available to measure mitochondrial Ca^{2+} efflux, and we find that some published protocols may induce mitochondrial permeability transition, underestimating the effects of these exchangers. In this work we describe a method to measure Na^{+} -sensitive and insensitive mitochondrial Ca^{2+} efflux activity in isolated mitochondria and permeabilized cells using the Ca^{2+} Green indicator and a fluorimeter. A checklist is provided to avoid artefacts as well as pinpoint adaptations necessary in specific experimental models.

1. Introduction

Mitochondria are metabolic and signalling hubs, essential players in the life and death of eukaryotic cells (Spinelli, Haigis 2018; Giacomello et al 2020). Their ability to take up, store, and release calcium (Ca^{2+}) in a regulated manner helps shape spatiotemporal features of Ca^{2+} signalling events (Rizzuto et al 2012). The presence of small and transient amounts of Ca^{2+} within mitochondria physiologically regulates both oxidative phosphorylation and the production of oxidants, but can also mediate mitochondrial damage when in excessive amounts (Rossi et al 2019; Vercesi et al 2018; Vilas-Boas et al 2022). Mitochondrial Ca^{2+} uptake and release take place through independent pathways, and both activities are supported by the proton motive force (Giorgi et al 2018).

The MCU complex (MCUc) is the most active pathway for Ca^{2+} uptake (Figure 1) (Feno et al 2021). Conversely, three main pathways have been described for Ca^{2+} efflux (Giorgi et al 2018): i) a $\text{Ca}^{2+}/\text{H}^+$ exchanger, the protein nature of which still lacks in consensus; ii) the sodium (Na^+) / lithium (Li^+) / Ca^{2+} exchanger (NCLX) that mediates Na^+ -dependent Ca^{2+} release (Palty et al 2010); and iii) the mitochondrial permeability transition pore (mPTP), which is a high conductance pathway that unselectively releases small molecules, including Ca^{2+} . mPTP is commonly induced by mitochondrial Ca^{2+} overload and oxidative imbalance (Figure 1) (Vercesi et al 2018).

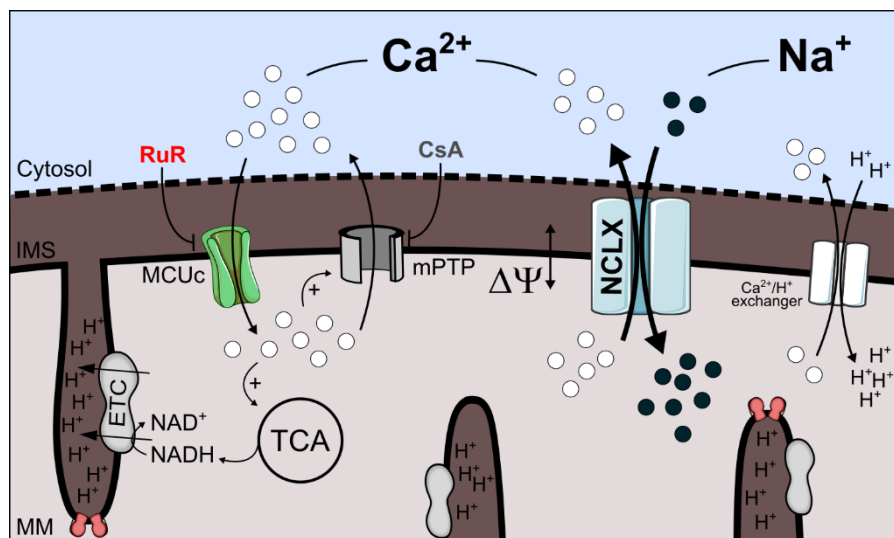


Figure 1. Mitochondrial Ca^{2+} transport pathways. Ca^{2+} entry into the mitochondrial matrix (MM) is mediated by the MCU complex (MCUc), a ruthenium red (RuR)-sensitive pathway. Ca^{2+} stimulates tricarboxylic acid (TCA) cycle dehydrogenases and inner mitochondrial membrane substrate transport. Ca^{2+} overload stimulates the formation of a high conductance pathway for Ca^{2+} efflux: the cyclosporin A (CsA)-inhibited mitochondrial permeability transition pore (mPTP). $\text{Ca}^{2+}/\text{H}^+$ and $\text{Na}^+/\text{Li}^+/\text{Ca}^{2+}$ (NCLX) exchangers avoid Ca^{2+} overload under physiological conditions. Both pathways depend on the proton electrochemical gradient.

Na^+ -dependent mitochondrial Ca^{2+} efflux through NCLX has emerged as an important regulator of different cellular processes and may be a promising therapeutic target for diseases such as cancer (Pathak et al 2020) and Alzheimer's (Jadiya P et al

2019). Thus, reliable protocols to test modulators of NCLX activity as well as to investigate changes in its function are needed. A comprehensive protocol would distinguish different efflux pathways, and can be used for *in vivo* and *in vitro* studies.

Here, we briefly discuss the current pros and cons of available protocols to measure mitochondrial Ca^{2+} efflux and provide a step-by-step protocol to assess Ca^{2+} efflux rates in isolated mitochondria or in permeabilized cells, focusing mainly on the activity of NCLX. We also discuss some important experimental precautions that are essential to achieve reliable measurements.

1.1. Mitochondrial Ca^{2+} transport measurement in intact cells

In experiments using intact cells, Ca^{2+} concentrations ($[\text{Ca}^{2+}]$) are commonly assessed through imaging methods using either genetically encoded (Cameleons, Pericams, Aequorins, etc) or exogenous Ca^{2+} probes (such as acetoxymethyl esters of Fura 2 or Ca^{2+} GreenTM-5N), some of which can uncover Ca^{2+} signalling events at the subcellular level (Whitaker 2010; Gryniewicz et al 1985; Minta et al 1989; Rudolf et al 2003). The free $[\text{Ca}^{2+}]$ in each cell compartment is the result of the balance between Ca^{2+} uptake, efflux, binding to chelators, and the formation of precipitates (Williams et al 2013).

Mitochondrial Ca^{2+} transport (uptake and efflux) is often studied measuring cytoplasmic and matrix $[\text{Ca}^{2+}]$ during a signalling event. Although this approach does measure mitochondrial Ca^{2+} transport in a more physiological state, the complexity of the system does not always allow for accurate determinations of sources and mechanisms in which changes occur. Modulation of endoplasmic reticulum (ER) Ca^{2+} stores or the activity of plasma membrane Ca^{2+} transporters may alter cytoplasmic signals independently of mitochondrial ionic transport. Indeed, Ca^{2+} levels in the mitochondrial matrix are determined by several factors that involve mitochondrial Ca^{2+} uptake and extrusion properties, the proximity with the ER or plasma membrane, their ability to buffer or precipitate Ca^{2+} , and the matrix volume, among other factors (de Brito, Scorrano 2008; Nita et al 2012; Kuo et al 2019; Kowaltowski et al 2019). Notably, the formation of Ca^{2+} precipitates in the matrix makes it difficult to obtain true measurements of Ca^{2+} flux using these techniques, as it underestimates total uptake into the organelle. Other limitations in whole cell measurements involve difficulties with the use of pharmacological inhibitors, which often have off-target effects.

1.2. Assessment of mitochondrial Ca^{2+} transport in isolated mitochondrial preparations

A more reductionist approach to study Ca^{2+} transport using isolated mitochondrial samples solves several of the pitfalls mentioned above, although it does not, of course, uncover conditions *in situ*. On the other hand, the mitochondrial microenvironment can be tightly controlled with isolated preparations, including the availability/concentration of substrates, inhibitors, and ions (Na^+ , Ca^{2+} and Li^+). Modulators such as ruthenium red (RuR – an MCU inhibitor) or CGP-37157 (CGP – an NCLX inhibitor) can dissect effects of uptake and efflux pathways (Cox et al 1993).

Mitochondrial isolation from organs, tissues or cell cultures relies on differential centrifugation and/or the use of density gradients (Gnaiger et al 2020a, 2020b). Mitochondrial isolation from cell cultures can be laborious and require large amounts of cells; in these models permeabilized cell protocols are a more suitable option, as

discussed below. Isolation of mitochondria from organs is easier and in general gives good yields. While the reductionist approach using isolated mitochondria facilitates specific measurements and decreases artifacts, the physiological relevance of this approach is limited, and several caveats should be noted (Gnaiger et al 2020a, 2020b; Schmidt et al 2021), including that the mitochondrial population is biased, as swollen mitochondria may be lost during isolation, and the composition of the media does not truly reflect the cytoplasm. Several cytoplasmic components, such as proteins and metabolites, are essential regulators of mitochondrial function. In isolated brain mitochondria, for example, the absence of adenine nucleotides deeply impairs their ability to take up and store Ca^{2+} . In such cases, it is important to add ADP/ATP to the buffer (Kristian et al 2002; Amigo et al 2017). Finally, morphology and interactions with other cell components, such as membranes and cytoskeleton, are expectedly lost in isolated mitochondrial preparations.

Because of Ca^{2+} precipitation in the matrix, which leads to underestimation of total uptake when using intramitochondrial probes, extracellular Ca^{2+} probes can be more accurate choices to measure mitochondrial Ca^{2+} fluxes. Mitochondrial Ca^{2+} uptake assays to determine entry rates as well as uptake capacity are more frequently performed than efflux assays (examples can be seen in Amigo et al 2017; Serna et al 2020; Serna et al 2022). While quite straightforward, authors should note that the fluorescence of extramitochondrial probes can be influenced by media composition, making calibration under different conditions essential (Rudolf et al 2003).

Mitochondrial efflux assays are less commonly performed and have the added difficulty that distinguishing between the different pathways ($\text{Ca}^{2+}/\text{H}^+$, NCLX or mPTP) may be tricky. The main problems with measurements of $\text{Ca}^{2+}/\text{H}^+$ and NCLX activity, in our hands, are related to the masking effect of mPTP induction. As mitochondria must be loaded with Ca^{2+} in order to measure extrusion, permeability transition is often induced in at least a subset of the mitochondrial population, as we will show below. Since Ca^{2+} efflux through the exchangers is supported by protonmotive force, mPTP formation hampers the detection of the activity of both exchangers (Haworth et al 1980, Boyman et al 2013; Giorgi et al 2018).

1.3. Assessment of mitochondrial Ca^{2+} transport in permeabilized cells

Permeabilized cell models represent a midway option between intact cell studies and isolated mitochondrial approaches (Fiskum et al 1980). While they preserve cell architecture and the relationship between some organelles, they allow for direct control and access to the mitochondrial microenvironment, including precise Ca^{2+} uptake and release measurements using extramitochondrial Ca^{2+} sensors. Permeabilization is promoted by using substances such as digitonin, α -tomatin, or saponin to disrupt the integrity of the plasma membrane, preserving mitochondrial membranes, as well as mitochondrial morphology, interactions with other cell components, and function. This is achieved by titration of these detergents, and using the fact that mitochondria are poor in cholesterol (Fiskum et al 1980; Fiskum et al 2000; Vercesi et al 1991; Kuznetsov et al 2008; Saks et al 1998). Plasma membrane permeabilization establishes a continuity between the cytoplasm and the extracellular medium, allowing for experiments that modulate mitochondrial function directly, and avoiding any limitation imposed by the plasma membrane for substrate, inhibitor, or ion availability. Additional ion transport

activities exerted by non-mitochondrial membranes such as the ER are also excluded by permeabilization, or using specific inhibitors as controls.

2. Mitochondrial Ca^{2+} efflux – isolated mitochondria

Isolated mitochondria may be obtained using many different protocols, and choices depend largely on the experimental model being studied. Here, we isolated mitochondria from mouse liver, as described previously (Tahara et al 2009, with modifications) and detailed below.

2.1. Liver Mitochondrial isolation

Animal procedures were conducted in accordance with guidelines from the Ethical Committee for Animal Research (CEUA-IQ/USP 196/2021). Animals were anaesthetised, euthanised, and had their livers immediately dissected. Mitochondria were isolated as follows:

1. Transfer the dissected liver to a beaker containing approximately 50 mL ice-cold phosphate buffered saline (PBS) (Table 1). Keep all subsequent materials and solutions over ice.
2. Thoroughly mince the tissue into small fragments, using sharp scissors. Alternatively, a polytron grinder may be used to get more homogeneous suspension, and smaller organ fragments.
3. Wash repeatedly to remove excess contaminating blood.
4. Remove the buffer and add 60 mL ice-cold isolation buffer (Table 2).
5. Using an electric Potter-Elvehjem tissue grinder, homogenize the tissue (approximately five to six strokes, or until the tissue is clearly dissociated).
6. Centrifugation #1 (remove cellular debris and blood): centrifuge at 900 x g, at 4°C, for 4 min.
7. Transfer the supernatant to a new tube, discarding the pellet.
8. Centrifugation #2: repeat steps 6 and 7.
9. Centrifugation #3 (pellet mitochondria): centrifuge supernatant at 9,000 x g, at 4°C, for 5 min.
10. Discard the supernatant and resuspend the pellet in 60 mL ice-cold isolation buffer (Table 2).
11. Centrifugation #4 (wash the pellet): centrifuge the suspension at 9,000 x g, at 4°C, for 5 min. Resuspend in 60 mL ice-cold resuspension buffer (Table 3).
12. Centrifugation #5 (remove BSA from samples): centrifuge resuspension at 9,000 x g, at 4°C, for 10 min.
13. Resuspend pellet in 300 μL ice-cold resuspension buffer (Table 3).
14. Maintain isolated mitochondria over ice to avoid degradation.
15. Measure protein concentrations using the Bradford method.

2.2. Defining ideal substrates by measuring Ca^{2+} retention capacity (CRC)

Before proceeding with mitochondrial Ca^{2+} efflux assessment *per se*, it is of interest to determine the optimal conditions for your given experimental model. The ability to take up and store Ca^{2+} varies greatly depending on the organ or cells from which the mitochondria originated. The chosen energizing substrate(s) also deeply influences the maximal amount of Ca^{2+} that can be taken up by mitochondria, before overt mitochondrial

permeability transition pore (mPTP) induction. This upper limit of Ca²⁺ uptake ability is known as Ca²⁺ retention capacity (CRC). In kidney mitochondria, for example, lower CRCs are observed when pyruvate and malate (which energize mitochondria mainly through complex I) are employed as substrates, relative to succinate plus rotenone (which fuels electron transport mainly through complex II) (Serna et al 2022). Defining the optimal substrates involves measuring mitochondrial CRC under each condition. Ca²⁺ uptake assays are performed as shown in [Figure 2](#), and described below.

1. Prepare the cuvette

1.1 Use a cuvette fluorimeter with stirring and temperature control. Select an appropriate cuvette. For standard-sized 2 mL cuvettes, add 2 mM pyruvate plus 2 mM malate (or 2 mM succinate plus 1 μM rotenone), 15 μM EGTA, and 75 nM Calcium Green™-5N in 2 mL experimental buffer ([Table 4](#)).

Note: the pH of substrates and EGTA needs to be adjusted to 7.2 using KOH when preparing the stock solutions.

1.2 Place the cuvette in the fluorimeter, with constant stirring, at 37°C.

1.3 Wait a couple of minutes until the buffer temperature and composition is homogeneous.

1.4 Start measuring fluorescence at $\lambda_{\text{ex}} = 506 \text{ nm}$ and $\lambda_{\text{em}} = 532 \text{ nm}$. Fluorimeter slits (or lamp voltage) should be adjusted to avoid saturation of the system.

2. Ca²⁺ loading traces to determine Ca²⁺ retention capacities

2.1 Add 0.5-1 mg of mitochondria and wait around 100 s for equilibration.

2.2 Perform sequential additions 10 μM CaCl₂, waiting approximately 300 s between them or until the Ca²⁺ bolus is completely taken up by mitochondria. Usually, because of the EGTA present, a few CaCl₂ additions need to be made at the beginning of each trace before you observe Ca²⁺ uptake (marked by a decrease in the Calcium Green fluorescence; true Ca²⁺ uptake exhibits an exponential-like decay shape, [Figure 2](#)).

2.3 Proceed with additions until you reach widespread mPTP opening in the mitochondrial population, indicated by the increase in fluorescence in the absence of added Ca²⁺ boluses, or until fluorescence stabilizes after Ca²⁺ additions, with no further measurable mitochondrial uptake.

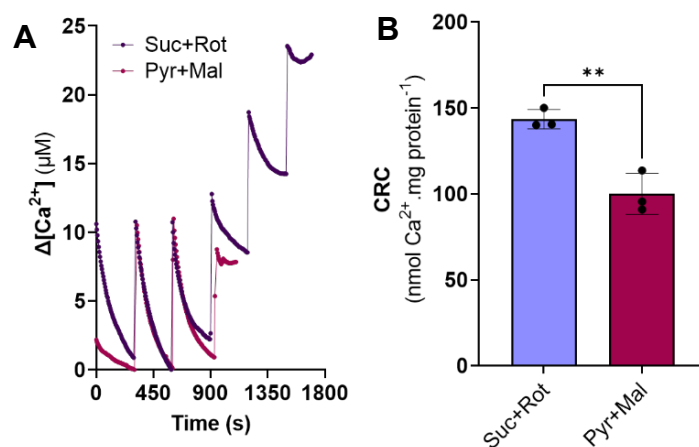


Figure 2. Ca²⁺ retention capacities in isolated mouse liver mitochondria: effect of different substrates. 500 μg liver mitochondria were incubated in 2 mL experimental

buffer using either succinate plus rotenone (Suc+Rot) or pyruvate plus malate (Pyr+Mal) as substrates. Extramitochondrial $[Ca^{2+}]$ were recorded over time using Calcium Green-5N. **(A)** Typical Ca^{2+} uptake trace. Each peak in the trace results from the sequential addition of $10 \mu M$ $CaCl_2$ boluses in the media. The subsequent decrease in extramitochondrial $[Ca^{2+}]$ results from Ca^{2+} uptake into the matrix. When the ability to take up and store Ca^{2+} is surpassed, $[Ca^{2+}]$ in the media no longer decreases. **(B)** Quantified Ca^{2+} retention capacities (CRC), or the total amount of Ca^{2+} taken up per mg mitochondrial protein over the full loading trace, obtained from traces such as panel A. CRCs are higher when succinate (plus rotenone) is employed as substrate. ****p < 0.01.**

2.3. Measuring mitochondrial Ca^{2+} efflux

Given the results seen in Figure 2, we chose succinate plus rotenone as the optimal energizing condition to measure Ca^{2+} efflux rates in liver mitochondria. We can now proceed to conduct Ca^{2+} efflux measurements.

Choosing Ca^{2+} loads for efflux measurements: avoiding mPTP opening

For obvious reasons, mitochondria must be loaded with Ca^{2+} to measure efflux rates, and different Ca^{2+} loads may generate different efflux rates. mPTP opening, which is bolstered by higher Ca^{2+} loads, will interfere with exchanger activity measurements, as it eliminates or decreases inner membrane potentials. It should, thus, be avoided when measuring Ca^{2+}/H^+ exchanger and NCLX activities. Widespread mPTP formation is easily identifiable when measuring Ca^{2+} fluxes, as it leads to overt Ca^{2+} release, but we find it can often be overlooked when affecting a subset of the mitochondrial population, as exemplified by the results in Figure 3. In it, mitochondria were loaded with three different amounts of Ca^{2+} , and subsequent extrusion rates were measured in the absence or presence of mPTP inhibitor cyclosporin A (CsA). We find that CsA-insensitive Ca^{2+} efflux (Ca^{2+}/H^+ efflux, in this instance, since Na^+ was not added) is similar under all conditions tested. However, total efflux rates increase with increasing Ca^{2+} loads due to a CsA-sensitive activity, which indicates that the mPTP was responsible. These results demonstrate that using higher Ca^{2+} loads promotes mPTP opening even when the CRC has not been exceeded.

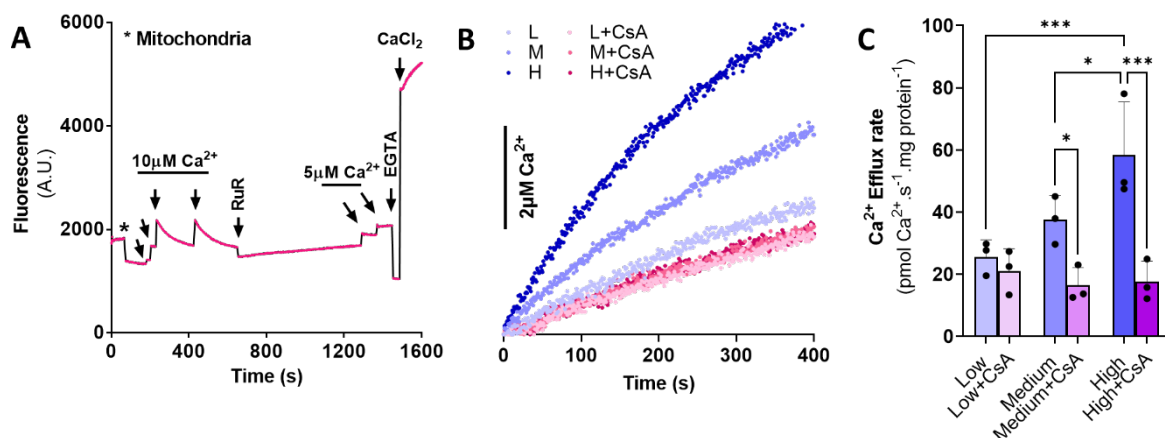


Figure 3. Permeability transition in mitochondrial subpopulations affects Ca^{2+} efflux measurements. 500 μg liver mitochondria were incubated in 2 mL experimental buffer with 2 mM succinate plus $1 \mu M$ rotenone. Extramitochondrial Ca^{2+} concentrations

were recorded using Calcium Green. **(A)** Representative plot for the full Ca²⁺ efflux assay, following Calcium Green fluorescence over time. Mitochondria were added (*) and allowed to equilibrate. The first two 10 μM CaCl₂ additions did not result in ion uptake as the chelator EGTA was present, as discussed [above](#). The gradual decrease in fluorescence observed after the third and fourth CaCl₂ additions is due to mitochondrial Ca²⁺ uptake. After the 40 nmol Ca²⁺ load, ruthenium red (RuR) was added, resulting in a small immediate fluorescence quenching. The slow increase in fluorescence that follows results from mitochondrial Ca²⁺ efflux. After several minutes recording this efflux, two sequential additions of 5 μM CaCl₂ were performed for calibration purposes. Along with this, minimal and maximal fluorescence values were determined by the addition of 1.5 mM EGTA and 10 mM CaCl₂, respectively. **(B)** Representative Ca²⁺ efflux traces; initially, mitochondria were loaded either with low (L~10 μM), medium (M~20 μM) or high (H~30 μM) amounts of Ca²⁺, in the presence or absence of 5 μM cyclosporin A (CsA). To measure mitochondrial Ca²⁺ efflux, ruthenium red (RuR) was added to the media at time = 0, and extrusion traces were followed over time. **(C)** Initial Ca²⁺ efflux rates were determined as the slope of the linear portion of the efflux trace just after RuR addition. *p < 0.05; **p < 0.01; ***p < 0.005.

Measuring mPTP- and Na⁺-independent mitochondrial Ca²⁺ efflux

We established that the CsA-sensitive efflux rate under our conditions was not significant when 40 nmol Ca²⁺/mg mitochondrial protein were employed as a calcium load, and used this condition to study exchanger-dependent Ca²⁺ efflux, as follows:

1. Add 0.5-1 mg of mitochondria to a fluorimeter cuvette and media containing Calcium Green as described in uptake experiments above. Wait around 100 s for equilibration.
 - Note:** experimental modulators of mitochondrial activity, such as CsA, should be added before mitochondria. If a low enough Ca²⁺ load to avoid mPTP opening cannot be achieved, CsA may be used in all traces.
2. Add 10 μM CaCl₂ and wait for fluorescence to stabilize after Ca²⁺ is taken up.
 - Note:** sequential additions may be needed to overcome EGTA chelation. Assessing the activity of Ca²⁺ exchangers requires Ca²⁺ load optimization to avoid mPTP opening (see critical point [above](#)).
3. Add 1-2.5 μM RuR (or another MCU inhibitor) to inhibit mitochondrial Ca²⁺ uptake.
 - Note:** final RuR concentrations should be titrated. In liver, kidney, and heart mitochondria, we find this concentration range works well.
4. Record Ca²⁺ efflux during at least 400 s.

Measuring Na⁺-dependent mitochondrial Ca²⁺ efflux

The protocol to assess Na⁺(or Li⁺)-stimulated Ca²⁺ efflux is essentially the same as that to measure basal Ca²⁺ efflux, but with added Na⁺:

1. Repeat steps 1-3 [above](#).
2. After Ca²⁺ loading and inhibition of the MCU with RuR, allow the system to equilibrate for 100-200s.
3. Add 20 mM NaCl (or LiCl) to induce a Na⁺(Li⁺)-dependent Ca²⁺ efflux. Record fluorescence changes for at least 400 s.

Note: Ca^{2+} efflux rates must be calculated and compared using the same initial and final time points: matrix Ca^{2+} concentrations decrease over time, and efflux rates do too.

- To estimate NCLX-dependent efflux, subtract the basal efflux rate from the efflux after Na^+ stimulation.

Figure 4 shows an example in which Ca^{2+} efflux rates were measured in isolated mouse liver mitochondria. We observed significant and similar Na^+ and Li^+ stimulation of Ca^{2+} efflux under these conditions, indicating the presence of NCLX activity, corresponding to more than half of the total extrusion activity in these mitochondria. Our results contrast with those of other authors, who were unable to observe Na^+ -stimulated efflux in liver mitochondria (Rysted et al 2021), possibly due to mPTP induction, given a high Ca^{2+} load was employed. Indeed, Haworth et al (1980) reported similar Na^+ -stimulated efflux values to those we obtained.

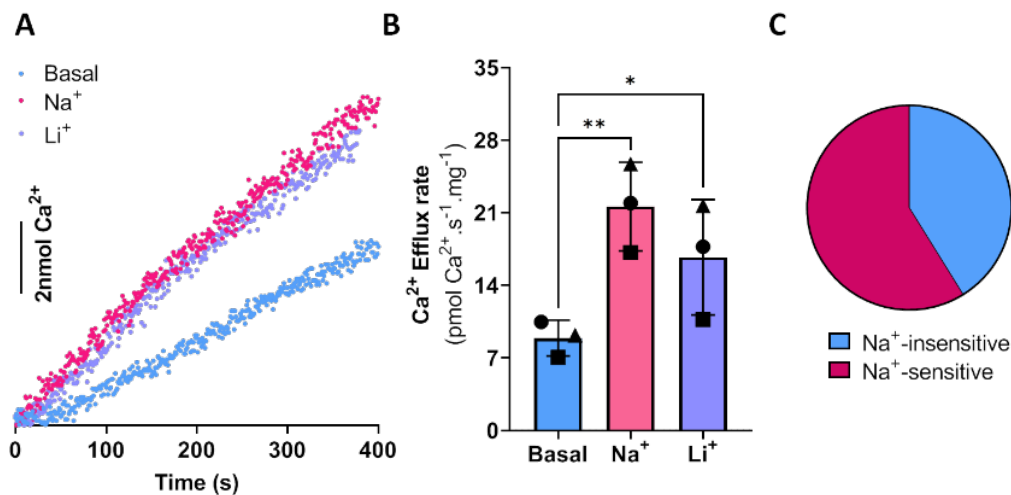


Figure 4. Ca^{2+} efflux in mouse liver mitochondria. 1 mg liver mitochondria was incubated in 2 mL experimental buffer with 2 mM succinate plus 1 μM rotenone. Extramitochondrial Ca^{2+} was recorded using Calcium Green. (A) Typical Ca^{2+} extrusion traces. Mitochondria were loaded with 40 nmol Ca^{2+} , as shown for Figure 3, and then treated with 2.5 μM RuR at time = 0. Ca^{2+} efflux was measured under basal conditions or stimulated with 20 mM Na^+ or Li^+ , as indicated. (B) Ca^{2+} efflux rates were determined from the slope just after Na^+ or Li^+ additions. (C) Relative contribution of Na^+ -sensitive and Na^+ -insensitive Ca^{2+} efflux pathways.

Calibration: transforming Calcium Green fluorescence into $[\text{Ca}^{2+}]$

Fluorescence changes of the Calcium Green probe should be transformed into $[\text{Ca}^{2+}]$ by calibrating. We find that the addition of some mitochondrial modulators and ions alters probe response to changes in $[\text{Ca}^{2+}]$, so calibrations should be conducted separately for each experimental condition, as follows (see a sample trace in Figure 3A):

- At the end of each experimental trace, make at least two consecutive additions of 5 μM CaCl_2 to the experimental media while recording Calcium Green fluorescence.
- Add 1.5 mM EGTA (or more, if necessary) to achieve minimal Calcium Green fluorescence (F_{\min}).

3. Add 10 mM CaCl₂ (or more, if necessary) to reach maximal Calcium Green (F_{max}).
4. K_d calculation: The K_d is empirically determined as the value in which the change in fluorescence (ΔF) before and after Ca²⁺ additions fits the 5 μM Ca²⁺ increase. This process is made by iteration, as follows:
 - Covert all fluorescence values to [Ca²⁺] according to the equation $[Ca^{2+}] = K_d \cdot (F - F_{min}) / (F_{max} - F)$ by using a pre-determined K_d value (e.g. 50 μM).
 - Calculate the Δ[Ca²⁺] from before and after the 5 μM CaCl₂ additions.
 - Decrease or increase the K_d value in the formula until the Δ[Ca²⁺] value is equal to 5 μM (iteration).
5. Calculate calcium concentrations for the experimental traces using the K_d value obtained and the formula: $[Ca^{2+}] = K_d \cdot (F - F_{min}) / (F_{max} - F)$.

3. Mitochondrial Ca²⁺ efflux – permeabilized cells

Permeabilized cells allow for assessments using protocols similar to those used for isolated mitochondria, once optimal permeabilization conditions are established. We exemplify here using human hepatoma PLC/PRF/5 cells.

3.1. Digitonin titration for optimal permeabilization

We employed digitonin to selectively permeabilize cell membranes without disturbing mitochondrial integrity. Optimal digitonin concentrations were determined using an Oroboros high-resolution oxygraph. The titration assay relies on the low permeability of the plasmalemma to succinate, a restraint removed when the membrane is permeabilized, resulting in increased mitochondrial oxygen consumption rates in the presence of rotenone. ADP is commonly added to increase respiration and titration sensitivity. A detailed digitonin titration protocol is:

1. Prepare the cell suspension

- 1.1 Plate cells to obtain > 1 · 10⁶ cells at the desired confluence (e.g., a 100 mm culture dish per trace).
- 1.2 Wash cells with warm PBS.
- 1.3 Add 2 mL of trypsin-EDTA solution and incubate at 37°C for 3-5 min (depending on cell type).
- 1.4 Inhibit trypsin with 4 mL culture media.
- 1.5 Collect cells and centrifuge at 1200 rpm for 5 min.
- 1.6 Wash cells: resuspend in 4 mL experimental buffer supplemented with 1 mM EGTA.
- 1.7 Mix gently with a widened (cut) 1000 μL pipette tip to disaggregate any cell clumps.
- 1.8 Centrifuge the cell suspension at 1200 rpm for 5 min.
- 1.9 Resuspend cells in 500 μL experimental buffer with 1 mM EGTA. Dilute the cell suspension (if required) and count viable cells.

Note: when cells have a strong tendency to form clumps, dilute the cells with PBS supplemented with EGTA and EDTA before counting.

2. Titrating digitonin concentrations

- 2.1 Add 2 mM succinate, 1 μM rotenone, and 1 mM ADP to experimental buffer in an Oroboros high-resolution oxygraph chamber.

- 2.2 Add the cell suspension for a final concentration of $0.5 \cdot 10^6$ cells/mL in 2 mL experimental buffer (supplemented 1 mM EGTA).
- 2.3 Make sequential 0.5% digitonin additions (aim for incremental additions of 0.5-1 μ L) and observe oxygen consumption increase, then gradually decrease again (Figure 5).
Note: allow the system to properly equilibrate. Initial additions are more time-demanding. Wait between 2-6 minutes between digitonin additions.
- 2.4 Optimal digitonin concentrations will be those that induce highest mitochondrial respiration.

3. Outer mitochondrial membrane integrity assay

To validate cell permeabilization quality, a control for outer mitochondrial membrane integrity can be performed. Excessive amounts of digitonin lead to outer membrane permeabilization and subsequent cytochrome C release. Under these conditions, oxygen consumption rates are lower. Exogenous cytochrome C addition in the media recovers normal electron transport activity. The assay can be conducted as follows:

If cells have been properly permeabilized, no differences should be detected between respiratory rates in state 3 and state 3 + cytochrome C. As shown in (Figure 5), the chosen digitonin concentration does not induce outer mitochondrial membrane disruption.

- 3.1 Add 2 mM succinate and 1 μ M rotenone to experimental buffer in an Oroboros high-resolution oxygraph chamber, plus the chosen digitonin concentration.
- 3.2 Add the cell suspension at a final concentration of $0.5 \cdot 10^6$ cells/mL.
- 3.3 Measure oxygen consumption in State 3: add 1 mM ADP.
- 3.4 Measure oxygen consumption in State 3 + cytochrome C: add 10 μ M cytochrome C.
- 3.5 Measure oxygen consumption in State 4: add 1 μ M oligomycin.
- 3.6 Measure non-mitochondrial respiration: add 1 μ M antimycin A.

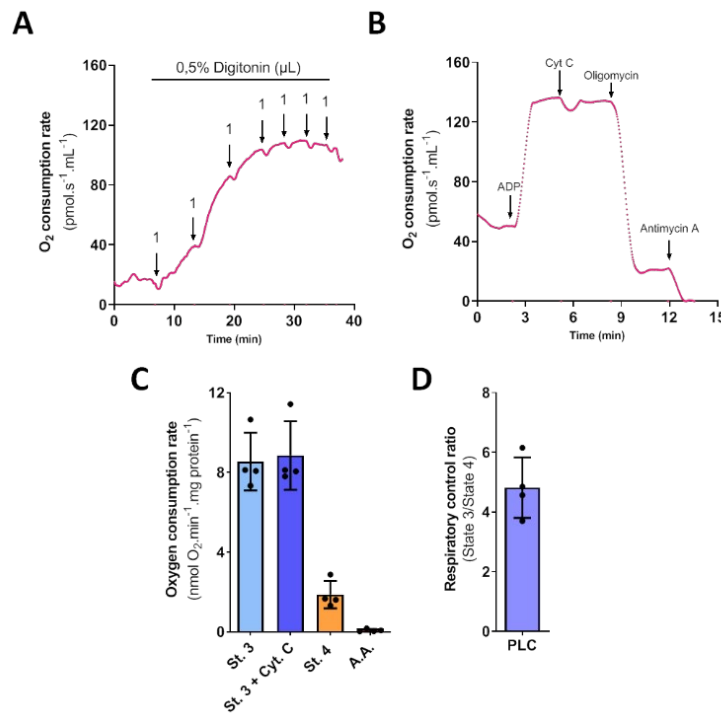


Figure 5. Optimization of cell permeabilization by digitonin. $1 \cdot 10^6$ PLC/PRF/5 cells were incubated in 2 mL experimental buffer the presence of 2 mM succinate and 1 μ M rotenone. Oxygen consumption rates were measured with a high resolution Oroboros oxygraph. **(A)** Titration: sequential additions of 1 μ L of 0.5% digitonin were made until respiratory inhibition was observed; 1 mM ADP was present from the beginning. **(B)** Representative trace for outer mitochondrial membrane integrity assessment using cytochrome C (cyt C) and $6.25 \cdot 10^{-3}$ % digitonin. 1 mM ADP, 10 μ M cytochrome C, 10 μ M oligomycin and 1 μ M antimycin A were added where indicated **(C)** Quantifications for traces such as in Panel B **(D)** Respiratory control ratios determined as the ratio between oxygen consumption rates in State 3 and State 4.

3.2. Define ideal substrates by measuring CRC

Follow the experiments described in section 2.2 to determine ideal substrates to use with your cell type.

3.3. Measuring mitochondrial Ca²⁺ efflux and assessing NCLX activity

Mitochondrial Ca²⁺ efflux assessment in permeabilized suspended cells follows similar protocols to those described for isolated mitochondria:

1. Prepare the cuvette

- 1.1 Add the chosen substrates and 20-40 μ M EGTA in experimental buffer (Table 4) plus 75 nM Calcium Green-5N and the optimal digitonin concentration, as defined above.

Note: modulators of mitochondrial function as CsA should be added before the cells.

- 1.2 Place the cuvette in the fluorimeter, with constant stirring, at 37°C.

- 1.3 Wait a couple of minutes until the buffer temperature and composition is homogeneous.
- 1.4 Start measuring fluorescence at $\lambda_{\text{ex}} = 506 \text{ nm}$ and $\lambda_{\text{em}} = 532 \text{ nm}$. Fluorimeter slits (or lamp voltage) should be adjusted to avoid saturation of the system.

2. Ca^{2+} loading

- 2.1 Add $1 \cdot 10^6$ cells and wait around 100 s for equilibration.
- 2.2 Add 10 μM (or 5 μM) CaCl_2 until cells have been uploaded with 20-30 nmol $\text{Ca}^{2+}/ 1 \cdot 10^6$ cells. Usually a few CaCl_2 additions must be made before Ca^{2+} uptake is observed.

Note: As discussed previously for isolated mitochondria preparations, low Ca^{2+} loads are necessary to avoid mPTP opening.

- 2.3 Add 2.5 μM RuR to inhibit mitochondrial Ca^{2+} uptake.

3. Mitochondrial Ca^{2+} efflux

- 3.1 Record Ca^{2+} efflux during at least 700 s to determine basal efflux rates.
- 3.2 Add 20 mM NaCl or LiCl to induce a $\text{Na}^+(\text{Li}^+)$ -dependent Ca^{2+} efflux, as shown in Figure 6.

Note: Ca^{2+} efflux rates must be calculated at equal time points, as discussed for isolated mitochondria.

- 3.3 Calibrate traces as described above.

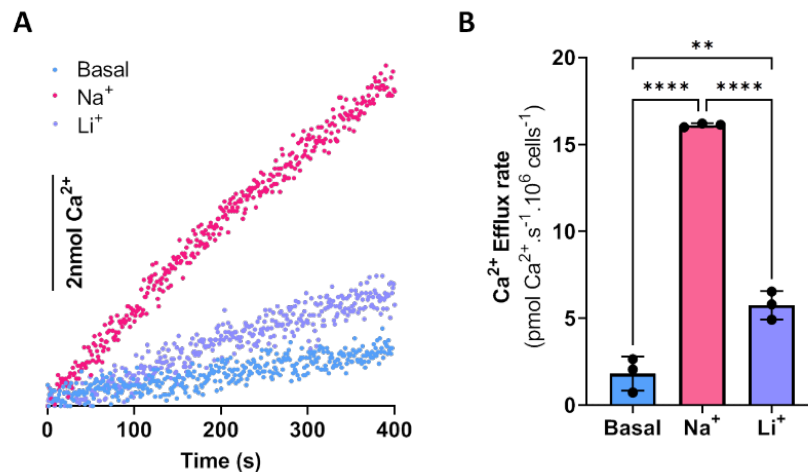


Figure 6. Mitochondrial Ca^{2+} efflux in permeabilized PLC cells. $1 \cdot 10^6$ PLC/PRF/5 cells were incubated in 2 mL buffer in the presence of 2 mM succinate, 1 μM rotenone and $6.25 \cdot 10^{-3}\%$ digitonin. Ca^{2+} efflux was recorded following Calcium Green fluorescence at 37°C . **A)** Representative Ca^{2+} efflux trace. Mitochondria were loaded with 20 nmol Ca^{2+} and then treated with 2.5 μM RuR at time = 0. Ca^{2+} efflux was measured under either basal conditions or stimulated with 20 mM Na^+ or Li^+ . **(B)** Ca^{2+} efflux rates were quantified from the slope of the linear portion of the efflux trace just after Na^+ or Li^+ additions (or 200s after RuR addition in the control group).

4. Calibration: transforming Ca^{2+} -Green fluorescence into $[\text{Ca}^{2+}]$

Fluorescence traces should be transformed into $[\text{Ca}^{2+}]$ measurements, as described in section 2.3. Experimental and calibration steps can be combined in the same trace, as shown in Figure 3A.

4. Protocol Validation and Reproducibility

To demonstrate the robustness of our protocols, we validated their applicability in two additional models: rat heart mitochondria and the INS-1E insulinoma cell line.

4.1. Isolated heart mitochondria

Total rat heart mitochondria were isolated using a protocol that includes both subsarcolemmal and intermyofibrillar mitochondria (Gotimskaya, Galkim 2010; Serna et al 2020). We then measured Ca²⁺ efflux rates as described above for liver mitochondria; results are presented in Figure 7. We find that the protocol is also appropriate for Ca²⁺ efflux measurements in heart mitochondria, and also confirm data from previous work (Rysted et al 2021) demonstrating that the Na⁺-sensitive pathway is predominant in heart, but that it is less stimulated by Li⁺.

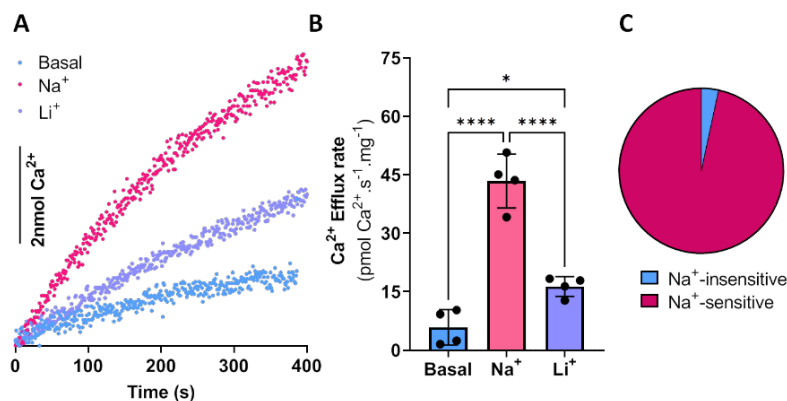


Figure 7. Ca²⁺ efflux in rat heart mitochondria. 500 µg of heart mitochondria were incubated in 2 mL experimental buffer in the presence of 2 mM succinate plus 1 µM rotenone. Extramitochondrial Ca²⁺ concentrations were recorded over time using Calcium Green-5N. (A) Typical Ca²⁺ release traces. Mitochondria were loaded with 20 nmol Ca²⁺ and then treated with 2.5 µM RuR at time = 0. Ca²⁺ efflux was measured under basal conditions or stimulated with 20 mM Na⁺ or Li⁺. (B) Ca²⁺ efflux rates were determined as the slope of the linear portion of the efflux trace just after Na⁺ or Li⁺ addition (or 200s after RuR addition in the control group). (C) Relative contribution of Na⁺-sensitive and Na⁺-insensitive Ca²⁺ efflux pathways. *p < 0.05; ****p < 0.001

4.2. Digitonin-permeabilized INS-1E cells

INS-1E cells were trypsinized, collected and counted as described previously for PLC/PRF/5 cells. Digitonin concentration was titrated and outer mitochondrial integrity controls were performed (Figure 8 A,B). Ca²⁺ efflux was assessed as in section 3.3 (Figure 8 C). As described for PLC cells, either Na⁺ or Li⁺ are able to stimulate Ca²⁺ efflux, demonstrating that the described protocol is adaptable to other cell types.

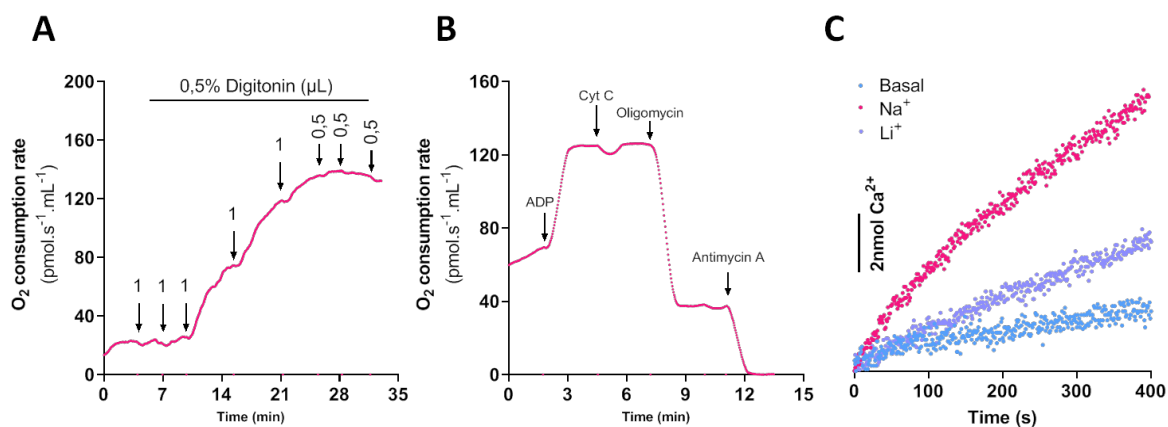


Figure 8. Digitonin titration and Ca^{2+} efflux measurements in permeabilized INS-1E cells. $2.5 \cdot 10^6$ INS-1E cells were incubated in 2 mL experimental buffer the presence of 2 mM succinate plus 1 μM rotenone. Oxygen consumption rates were measured with a high resolution oxygraph. **(A)** Titration 1 mM ADP was added in the media and sequential additions of 0.5 or 1 μL of 0.5% digitonin were made where indicated. **(B)** Representative trace for outer mitochondrial membrane integrity assessment using cytochrome C (cyt C). Mitochondrial activity was modulated by the sequential addition of 1 mM ADP, 10 μM cyt C, 10 μM oligomycin, and 5 μM antimycin A (A.A.). **(C)** Representative Ca^{2+} efflux trace. Mitochondria were loaded with 20 nmol Ca^{2+} and then treated with 2.5 μM RuR at time = 0. Ca^{2+} efflux was measured under basal conditions or stimulated with 20 mM Na^+ or Li^+ .

5. Troubleshooting

Problem	Possible reason	Solution
High basal (Na^+ -independent) Ca^{2+} efflux rates, or low Na^+ -sensitive Ca^{2+} efflux rates.	Mitochondrial permeability transition is being induced.	Decrease mitochondrial Ca^{2+} load or add cyclosporin A to avoid mPTP opening.
Ca^{2+} uptake/efflux trace is noisy	Mitochondrial clumps are present in isolated mitochondrial samples.	Gently disaggregate mitochondrial pellets using a brush with soft bristles.
	Cells are not properly dissociated, forming clumps. Cell culture trypsinization is insufficient.	Optimise trypsinization protocol for each cell type.
	Dead cells release DNA, promoting clump formation.	Decrease trypsinization time (or trypsin amount).
Cytochrome c stimulates state 3 oxygen consumption rates	Mitochondrial outer membrane permeabilization and cytochrome c release leads to electron transport impairment.	Decrease digitonin concentrations in the experimental medium.
Abundant cell clumps during counting	Cell-cell interactions are preserved after sample preparation; such interactions are favoured by Ca^{2+} and Mg^{2+} .	Dilute cell stocks in PBS supplemented with EDTA before counting.

6. Conclusion

We describe a method to measure Ca²⁺ efflux in isolated mitochondria and permeabilized cells, as indicated in the workflow in [Figure 9](#). Our approach allows us to dissect between Na⁺-sensitive and insensitive Ca²⁺ efflux. We demonstrate that a vital point in obtaining consistent and reliable Ca²⁺ extrusion activity measurements through mitochondrial exchangers is to avoid mPTP opening by either using low Ca²⁺ loads or adding cyclosporin A to all traces. In the absence of this step, at least part of the activity of NCLX and Ca²⁺/H⁺ exchange may be masked by mPTP-promoted permeabilization. Using this method, we were able to demonstrate NCLX activity in mouse liver mitochondria and permeabilized liver hepatoma PLC/PRF/5 cells. Additionally, we validated our method in isolated rat heart mitochondria, as well as the insulinoma cell line INS-1E.

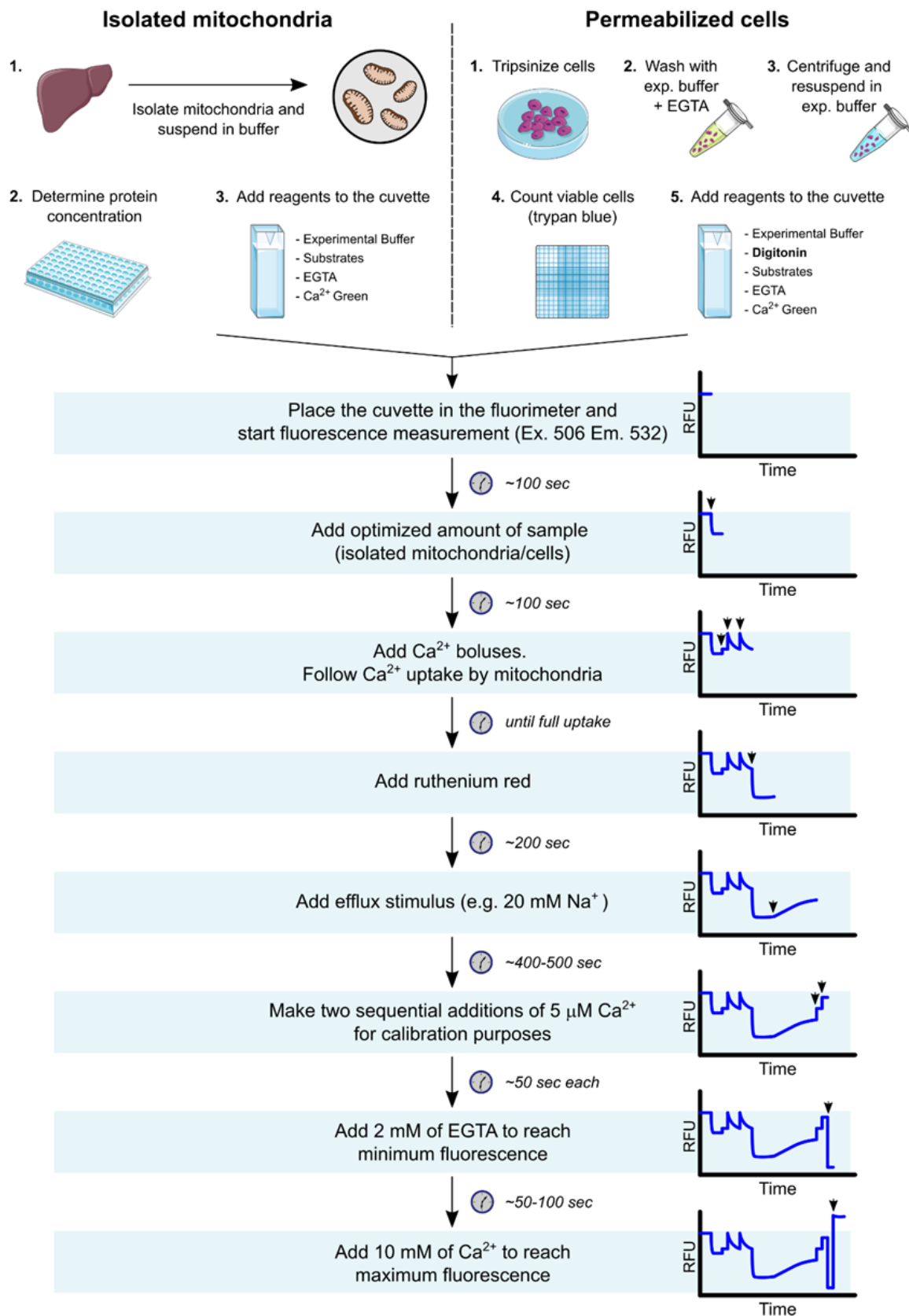


Figure 9. Schematic workflow for mitochondrial Ca²⁺ efflux measurements.

7. Annex: Media composition tables

Table 1. Phosphate buffered saline (pH = 7.4, adjusted with NaOH)

Reagent	Final concentration	Amount
NaCl	1.37 M	80.01 g
KCl	27 mM	2.01 g
Na ₂ HPO ₄	100 mM	14.2 g
KH ₂ PO ₄	18 mM	2.45 mg
EDTA	10 mM	3.8 g
milliQ H ₂ O	-	adjust to 1 L

Table 2. Liver isolation buffer (pH = 7.2, adjusted with KOH)

Reagent	Final concentration	Amount
Sucrose	250 mM	85.57 g
Hepes	10 mM	2.38 g
EGTA	1 mM	380 mg
EDTA	1 mM	380 mg
BSA (fatty-acid free)	1 mg/mL	1 g
milliQ H ₂ O	-	adjust to 1 L

Note: To avoid formation of bubbles or clumps when diluting BSA, add the powder over the solution and leave still for a while. Adjust pH only with KOH and HCl. Store at 4°C for up to a month.

Table 3. Resuspension buffer (pH = 7.2, adjusted with KOH)

Reagent	Final concentration	Amount
Sucrose	300 mM	20.54 g
Hepes	10 mM	476 mg
EGTA	2 mM	152 mg
milliQ H ₂ O	-	adjust to 200 mL

Store at 4°C for up to a month.

Table 4. Experimental buffer (pH = 7.2, adjusted with KOH)

Reagent	Final concentration	Amount
Sucrose	125 mM	21.39 g
KCl	65 mM	2.42 g
Hepes	10 mM	1.19 g
MgCl ₂	2 mM	95 mg
KH ₂ PO ₄	2 mM	136 mg
BSA (fatty acid-free)	0.1 mg/mL	50 mg
milliQ H ₂ O	-	adjust to 500 mL

To avoid formation of bubbles or clumps when diluting BSA, add the powder over the solution and leave it without stirring for a while. Store at 4°C for up to a month. Adjust pH only with KOH and HCl.

Abbreviations

Δp	protonmotive force	mPTP	mitochondrial permeability transition pore
$\Delta\Psi$	membrane potential	NCLX	Na ⁺ /Li ⁺ /Ca ²⁺ exchanger
ΔpH	pH gradient	RCR	respiratory control ratio
BSA	bovine serum albumin	RuR	Ruthenium Red
CGP	CGP-37157	St. 3	State 3
CRC	calcium retention capacity	St. 4	State 4
CsA	Cyclosporin A		
Cyt C	Cytochrome C		

Acknowledgements

The authors would like to acknowledge remarkable technical support by Sirlei Mendes de Oliveira, and excellent animal care lead by Sylvania Neves and Flavia Ong in the IQ-FCF/USP animal facility. This work was funded by grant #2020/06970-5 from the São Paulo Research Foundation (FAPESP), Centro de Pesquisa, Inovação e Difusão de Processos Redox em Biomedicina (CEPID Redoxoma, FAPESP grant #2013/07937-8), Conselho Nacional de Desenvolvimento Científico e Tecnológico (CNPq), and Coordenação de Aperfeiçoamento de Pessoal de Nível Superior (CAPES) line 001. Authors were supported by FAPESP fellowships #2017/14713-0 (JVCC), #2019/05226-3 (JDCS), #2019/18402-4 (VMR), #2021/02481-2 (EAVB), and #2021/13933-1 (GO). Parts of the figures were drawn by using pictures from Servier Medical Art. Servier Medical Art by Servier is licensed under a Creative Commons Attribution 3.0 Unported License (<https://creativecommons.org/licenses/by/3.0/>).

References

- Amigo I, Menezes-Filho SL, Luévano-Martínez LA, Chausse B, Kowaltowski AJ (2017) Caloric restriction increases brain mitochondrial calcium retention capacity and protects against excitotoxicity. *Aging Cell* 16:73-81. <https://doi.org/10.1111/ace.12527>
- Boyman L, Williams GSB, Khananshvil D, Sekler I, Lederer WJ (2013) NCLX: The mitochondrial sodium calcium exchanger. *J Mol Cell Cardiol* 59:205-13. <https://doi.org/10.1016/j.yjmcc.2013.03.012>
- Cox DA, Conforti L, Sperelakis N, Matlib MA (1993) Selectivity of inhibition of Na(+)-Ca²⁺ exchange of heart mitochondria by benzothiazepine CGP-37157. *J Cardiovasc Pharmacol* 21: 595-9. <https://doi.org/10.1097/00005344-199304000-00013>
- de Brito OM, Scorrano L (2008) Mitofusin 2 tethers endoplasmic reticulum to mitochondria. *Nature* 456: 605-10. <https://doi.org/10.1038/nature07534>
- Feno S, Rizzuto R, Raffaello A, Vecellio Reane D (2021) The molecular complexity of the mitochondrial calcium uniporter. *Cell Calcium* 93:102322. <https://doi.org/10.1016/j.ceca.2020.102322>
- Fiskum G, Craig SW, Decker GL, Lehninger AL (1980) The cytoskeleton of digitonin-treated rat hepatocytes. *Proc Natl Acad Sci USA* 77:3430-4. <https://doi.org/10.1073/pnas.77.6.3430>
- Fiskum G, Kowaltowski AJ, Andreyev AY, Kushnareva YE, Starkov AA (2000) Apoptosis-related activities measured with isolated mitochondria and digitonin-permeabilized cells. *Methods Enzymol* 322:222-34. [https://doi.org/10.1016/S0076-6879\(00\)22023-5](https://doi.org/10.1016/S0076-6879(00)22023-5)
- Giacomello M, Pyakurel A, Glytsou C, Scorrano L (2020) The cell biology of mitochondrial membrane dynamics. *Nat Rev Mol Cell Biol* 21:204-24. <https://doi.org/10.1038/s41580-020-0210-7>
- Giorgi C, Marchi S, Pinton P (2018) The machineries, regulation and cellular functions of mitochondrial calcium. *Nat Rev Mol Cell Biol* 19:713-30. <https://doi.org/10.1038/s41580-018-0052-8>
- Gnaiger E - MitoEAGLE Task Group (2020) Mitochondrial physiology. *Bioenerg Commun* 2020.1. <https://doi.org/10.26124/bec:2020-0001.v1>
- Gnaiger E (2020) Mitochondrial pathways and respiratory control. An introduction to OXPHOS analysis. *Bioenerg Commun* 2020.2. <https://doi.org/10.26124/bec:2020-0002>
- Gostimskaya I, Galkin A (2010) Preparation of highly coupled rat heart mitochondria. *J Vis Exp* 43:2202. <https://doi.org/10.3791/2202>
- Grynkiewicz G, Poenie M, Tsien RY (1985) A new generation of Ca²⁺ indicators with greatly improved fluorescence properties. *J Biol Chem* 260:3440-50. [https://doi.org/10.1016/S0021-9258\(19\)83641-4](https://doi.org/10.1016/S0021-9258(19)83641-4)
- Haworth RA, Hunter DR, Berkoff HA (1980) Na⁺ releases Ca²⁺ from liver, kidney and lung

- mitochondria. *FEBS Lett* 110:216-8. [https://doi.org/10.1016/0014-5793\(80\)80076-7](https://doi.org/10.1016/0014-5793(80)80076-7)
- Jadiya P, Kolmetzky DW, Tomar D, Di Meco A, Lombardi AA, Lambert JP, Luongo TS, Ludtmann MH, Praticò D, Elrod JW (2019) Impaired mitochondrial calcium efflux contributes to disease progression in models of Alzheimer's disease. *Nat Commun* 10:3885. <https://doi.org/10.1038/s41467-019-11813-6>
- Kowaltowski AJ, Menezes-Filho SL, Assali EA, Gonçalves IG, Cabral-Costa JV, Abreu P, Miller N, Nolasco P, Laurindo FRM, Bruni-Cardoso A, Shirihai OS (2019) Mitochondrial morphology regulates organellar Ca²⁺ uptake and changes cellular Ca²⁺ homeostasis. *FASEB J* 33:13176-88. <https://doi.org/10.1096/fj.201901136R>
- Kuo IY, Brill AL, Lemos FO, Jiang JY, Falcone JL, Kimmerling EP, Cai Y, Dong K, Kaplan DL, Wallace DP, Hofer AM, Ehrlich BE (2019) Polycystin 2 regulates mitochondrial Ca²⁺ signaling, bioenergetics, and dynamics through mitofusin 2. *Sci Signal* 12:eaat7397. <https://doi.org/10.1126/scisignal.aat7397>
- Kuznetsov AV, Veksler V, Gellerich FN, Saks V, Margreiter R, Kunz WS (2008) Analysis of mitochondrial function in situ in permeabilized muscle fibers, tissues and cells. *Nat Protoc* 3:965-76. <https://doi.org/10.1038/nprot.2008.61>
- Kristián T, Weatherby TM, Bates TE, Fiskum G (2002) Heterogeneity of the calcium-induced permeability transition in isolated non-synaptic brain mitochondria. *J Neurochem* 83:1297-308. <https://doi.org/10.1046/j.1471-4159.2002.01238.x>
- Minta A, Kao JPY, Tsien RY (1989) Fluorescent indicators for cytosolic calcium based on rhodamine and fluorescein chromophores. *J Biol Chem* 264:8171-8. [https://doi.org/10.1016/S0021-9258\(18\)83165-9](https://doi.org/10.1016/S0021-9258(18)83165-9)
- Nita II, Hershfinkel M, Fishman D, Ozeri E, Rutter GA, Sensi SL, Khananshvil D, Lewis EC, Sekler I (2012) The mitochondrial Na⁺/Ca²⁺ exchanger upregulates glucose dependent Ca²⁺ signalling linked to insulin secretion. *PloS one* 7:e46649. <https://doi.org/10.1371/journal.pone.0046649>
- Palty R, Silverman WF, Hershfinkel M, Caporale T, Sensi SL, Parnis J, Nolte C, Fishman D, Shoshan-Barmatz V, Herrmann S, Khananshvil D, Sekler I (2010) NCLX is an essential component of mitochondrial Na⁺/Ca²⁺ exchange. *Proc Natl Acad Sci USA* 107: 436-441. <https://doi.org/10.1073/pnas.0908099107>
- Pathak T, Gueguinou M, Walter V, Delierneux C, Johnson MT, Zhang X, Xin P, Yeast RE, Emrich SM, Yochum GS, Sekler I, Koltun WA, Gill DL, Hempel N, Trebak M. (2020) Dichotomous role of the human mitochondrial Na⁺/Ca²⁺/Li⁺ exchanger NCLX in colorectal cancer growth and metastasis. *Elife* 9: e59686. <https://doi.org/10.7554/eLife.59686>
- Rizzuto R, De Stefani D, Raffaello A, Mammucari C. (2012) Mitochondria as sensors and regulators of calcium signalling. *Nat Rev Mol Cell Biol*. 13:566-78. <https://doi.org/10.1038/nrm3412>
- Rossi A, Pizzo P, Filadi R (2019) Calcium, mitochondria and cell metabolism: A functional triangle in bioenergetics. *Biochim Biophys Acta Mol Cell Res. Molecular Cell Research* 1866:1068-78. <https://doi.org/10.1016/j.bbamcr.2018.10.016>
- Rudolf R, Mongillo M, Rizzuto R, Pozzan T (2003) Looking forward to seeing calcium. *Nat Rev Mol Cell Biol* 4: 579-586. <https://doi.org/10.1038/nrm1153>
- Rysted JE, Lin Z, Walters GC, Rauckhorst AJ, Noterman M, Liu G, Taylor EB, Strack S, Usachev YM (2021) Distinct properties of Ca²⁺ efflux from brain, heart and liver mitochondria: The effects of Na⁺, Li⁺ and the mitochondrial Na⁺/Ca²⁺ exchange inhibitor CGP37157. *Cell Calcium*. 96:102382. [doi: 10.1016/j.ceca.2021.102382](https://doi.org/10.1016/j.ceca.2021.102382).
- Saks VA, Veksler VI, Kuznetsov AV, Kay L, Sikk P, Tiivel T, Tranqui L, Olivares J, Winkler K, Wiedemann F, Kunz WS (1998) Permeabilized cell and skinned fiber techniques in studies of mitochondrial function in vivo. *Mol Cell Biochem* 184:81-100.
- Schmidt CA, Kelsey H, Fisher-Wellman, Darrell Neuffer P (2021) From OCR and ECAR to energy: Perspectives on the design and interpretation of bioenergetics studies. *J Biol Chem* 297:101140. <https://doi.org/10.1016/j.jbc.2021.101140>
- Serna JDC, Caldeira da Silva CC, Kowaltowski AJ (2020) Functional changes induced by caloric

- restriction in cardiac and skeletal muscle mitochondria. *J Bioenerg Biomembr* 52:269-77. <https://doi.org/10.1007/s10863-020-09838-4>
- Serna JDC, Amaral AG, Caldeira da Silva CC, Munhoz AC, Vilas-Boas EA, Menezes-Filho SL, Kowaltowski AJ (2022) Regulation of kidney mitochondrial function by caloric restriction. *Am J Physiol Renal Physiol* (in press) <https://doi.org/10.1152/ajprenal.00461.2021>
- Spinelli JB, Haigis MC (2018) The multifaceted contributions of mitochondria to cellular metabolism. *Nat Cell Biol* 20: 745–754. <https://doi.org/10.1038/s41556-018-0124-1>
- Tahara EB, Navarete FD, Kowaltowski AJ (2009) Tissue-, substrate-, and site-specific characteristics of mitochondrial reactive oxygen species generation. *Free Radic Biol Med* 46:1283-97. <https://doi.org/10.1016/j.freeradbiomed.2009.02.008>
- Vercesi AE, Bernardes CF, Hoffmann ME, Gadelha FR, Docampo R (1991) Digitonin permeabilization does not affect mitochondrial function and allows the determination of the mitochondrial membrane potential of *Trypanosoma cruzi* in situ. *J Biol Chem* 266: 14431-4.
- Vercesi AE, Castilho RF, Kowaltowski AJ, de Oliveira HCF, de Souza-Pinto NC, Figueira TR, Busanello ENB (2018) Mitochondrial calcium transport and the redox nature of the calcium-induced membrane permeability transition. *Free Radic Biol Med* 129:1-24. <https://doi.org/10.1016/j.freeradbiomed.2018.08.034>
- Vilas-Boas EA, Cabral-Costa JV, Ramos VM, da Silva CCC, Kowaltowski AJ (2022) Goldilocks calcium and the mitochondrial respiratory chain: too much, too little, just right. *Biorxiv*. <https://doi.org/10.1101/2022.04.12.488015>
- Williams GSB, Boyman L, Chikando AC, Khairallah RJ, Lederer WJ (2013) Mitochondrial calcium uptake. *Proc Natl Acad Sci USA* 110:10479-86. <https://doi.org/10.1073/pnas.1300410110>
- Whitaker, M (2010) Genetically encoded probes for measurement of intracellular calcium. *Methods Cell Biol* 99:153-82. <https://doi.org/10.1016/B978-0-12-374841-6.00006-2>

Copyright: © 2022 The authors. This is an Open Access preprint (not peer-reviewed) distributed under the terms of the Creative Commons Attribution License, which permits unrestricted use, distribution, and reproduction in any medium, provided the original authors and source are credited. © remains with the authors, who have granted MitoFit Preprints an Open Access publication license in perpetuity.

